Chinese Physics C

Measurement of J/ψ leptonic width with the KEDR detector *

A. G. Shamov[1,1)] [KEDR collaboration]

1 (Budker Institute of Nuclear Physics, 11, Lavrentiev prospect, Novosibirsk, 630090, Russia)

Abstract We report a new precise determination of the leptonic widths of the J/psi meson performed with the KEDR detector at the VEPP-4M e^+e^- collider. The measured values of the J/psi parameters are:

$$\Gamma_{ee} \times \Gamma_{ee}/\Gamma = 0.3323 \pm 0.0064\,(\text{stat.}) \pm 0.0048\,(\text{syst.})\,\text{keV},$$
$$\Gamma_{ee} \times \Gamma_{\mu\mu}/\Gamma = 0.3318 \pm 0.0052\,(\text{stat.}) \pm 0.0063\,(\text{syst.})\,\text{keV}.$$

Assuming $e\mu$ universality and using the table value of the branching ratios the leptonic $\Gamma_{\ell\ell} = 5.59 \pm 0.12\,\text{keV}$ width and the total $\Gamma = 94.1 \pm 2.7\,\text{keV}$ widths were obtained. We also discuss in detail a method to calculate radiative corrections at a narrow resonance.

Key words J/ψ meson, lepton width, full width

PACS 13.20.Gd, 13.66.De, 14.40.Gx

1 Introduction

The J/ψ meson is frequently referred to as a hydrogen atom for QCD. The electron widths Γ_{ee} of charmonium states are rather well predicted by potential models [1, 2]. The uncertainty in the QCD lattice calculations of Γ_{ee} gradually approaches the experimental errors [3]. The full and dileptonic widths of a hadronic resonance, Γ and $\Gamma_{\ell\ell}$, describe fundamental properties of the strong potential [4].

In this report we discuss the results of the J/ψ meson observation in leptonic decay channels. Study of the $e^+e^- \to J/\psi \to \ell^+\ell^-$ cross section as function of energy allows one to determine the leptonic width $\Gamma_{\ell\ell}$ and its product to the decay ratio $\Gamma_{ee} \times \Gamma_{\ell\ell}/\Gamma$ thus the total width Γ can be also found. The product $\Gamma_{ee} \times \Gamma_{\ell\ell}/\Gamma$ determines the peak cross section while the leptonic width $\Gamma_{\ell\ell}$ is contained in the interference wave magnitude. Due to smallness of the interference effect the experimental accuracy of the $\Gamma_{\ell\ell}$ determination is rather poor. However, the branching ratio $\mathcal{B}_{\ell\ell}$ is known with the accuracy of 0.7% from the cascade decay $\psi(2S) \to J/\psi\,\pi^+\pi^-$ thus we report the high precision results on $\Gamma_{ee} \times \Gamma_{ee}/\Gamma$ and $\Gamma_{ee} \times \Gamma_{\mu\mu}/\Gamma$ and use the $\Gamma_{\ell\ell}$ value to check the analysis consistency only.

The extraction of resonance parameters from the measured cross section requires the accurate accounting of radiative corrections. The Sec. 8.2.4 of the highly cited report [4] treats the radiative corrections to $e^+e^- \to J/\psi \to \ell^+\ell^-$ cross section in the way contradicting to that used in the experiments [5, 6] and our work [7] therefore me start with the discussion of this issue.

2 Radiative corrections to J/ψ production and decays

In virtually all experimental analyses it is assumed that the resonant contribution to the cross section of $e^+e^- \to J/\psi \to \ell^+\ell^-$ is proportional to the product $\Gamma_{ee} \times \Gamma_{\ell\ell}/\Gamma$ where Γ_{ee} and $\Gamma_{\ell\ell}$ are so called experimental partial widths [8] recommended to use by the Particle Data Group since 1990:

$$\Gamma_{\ell\ell} \equiv \mathcal{B}_{ll(n\gamma)} \times \Gamma = \frac{\Gamma_{\ell\ell}^{(0)}}{|1-\Pi_0|^2}, \qquad (1)$$

where $\mathcal{B}_{ll(n\gamma)}$ is the branching ratio as it is measuring experimentally, Γ_{ee}^0 is the lowest order QED partial width and Π_0 is the vacuum polarization operator excluding J/ψ contribution. In contrast, the Sec. 8.2.4 of Ref. [4] proposes that the resonant contribution is

1) E-mail: A.G.Shamov@inp.nsk.su

proportional to $\Gamma_{ee} \times \Gamma_{\ell\ell}^{(0)}/\Gamma = \Gamma_{ee}^0 \times \Gamma_{\ell\ell}/\Gamma$.

According to Ref. [9] the cross section of the single–photon annihilation $e^+e^- \to \ell^+\ell^-$ can be written in the form

$$\sigma = \int dx \frac{\sigma_0((1-x)s)}{|1-\Pi((1-x)s)|^2} f(s,x), \qquad (2)$$

where the $f(s,x)$ is calculated with a high accuracy, the $\Pi(s)$ represents the vacuum polarization operator and $\sigma_0(s)$ in the Born level cross section of the process.

Assuming the Breit-Wigner shape for σ_0

$$\sigma(s) = \frac{12\pi \Gamma_{ee}^0 \Gamma_{\ell\ell}^0}{(s-M^2)^2 + M^2\Gamma^2} \qquad (3)$$

and replacing $\Pi(s)$ with Π_0 mentioned above, one reproduces the result of the Sec. 8.2.4 of Ref. [4].

However, the Born level cross section of the $e^+e^- \to \ell^+\ell^-$ process is the smooth function of s therefore the resonance behavior of the cross section (2) is due to energy dependence of the full vacuum polarization operator Π containing the resonant contribution*. One has $\Pi = \Pi_0 + \Pi_R$ with nonresonant $\Pi_0 = \Pi_{ee} + \Pi_{\mu\mu} + \Pi_{\tau\tau} + \Pi_{q\bar{q}}$ and

$$\Pi_R(s) = \frac{3\Gamma_{ee}^0}{\alpha} \frac{s}{M_0} \frac{1}{s-M_0^2+iM_0\Gamma_0}, \qquad (4)$$

where M_0, Γ_0 and $\Gamma_{ee}^{(0)}$ are the "bare" resonance mass and widths.

The formula (2) gives the cross section without separation to the continuum, resonant and interference parts. To obtain the contribution of the resonance, the continuum one must be subtracted from the amplitude. It can be done with the equality

$$\frac{1}{1-\Pi_0-\Pi_R(s)} \equiv$$
$$\frac{1}{1-\Pi_0} + \frac{1}{(1-\Pi_0)^2} \frac{3\Gamma_{ee}^0}{\alpha} \frac{s}{M_0} \frac{1}{s-\tilde{M}^2+i\tilde{M}\tilde{\Gamma}} \qquad (5)$$

in which both $\tilde{M}$ and $\tilde{\Gamma}$ depend on s:

$$\tilde{M}^2 = M_0^2 + \frac{3\Gamma_{ee}^0}{\alpha} \frac{s}{M_0} \mathrm{Re}\, \frac{1}{1-\Pi_0},$$
$$\tilde{M}\tilde{\Gamma} = M_0\Gamma_0 - \frac{3\Gamma_{ee}^0}{\alpha} \frac{s}{M_0} \mathrm{Im}\, \frac{1}{1-\Pi_0}. \qquad (6)$$

In a vicinity of a narrow resonance this dependence is negligible thus the resonant contribution can be described with the Breit-Wigner amplitude containing "dressed" parameters $M \approx \tilde{M}(M_0^2)$, $\Gamma \approx \tilde{\Gamma}(M_0^2)$. Due to the extra power of the vacuum polarization factor $1/|1-\Pi_0|$ in the second term of (5) the resonant part

of the $e^+e^- \to \ell^+\ell^-$ cross section is proportional to $\Gamma_{ee} \times \Gamma_{\ell\ell}/\Gamma$ and does not depend on $\Gamma_{ee}^{(0)}$ explicitly.

The analytical expressions for the $e^+e^- \to \ell^+\ell^-$ cross section in the soft photon approximation were first derived by Ya. A. Azimov et al. in 1975 [10]. With some up-today modifications one obtains in the vicinity of a narrow resonance

$$\left(\frac{d\sigma}{d\Omega}\right)^{ee\to\mu\mu} \approx \left(\frac{d\sigma}{d\Omega}\right)_{\mathrm{QED}}^{ee\to\mu\mu} + \frac{3}{4M^2}(1+\delta_{\mathrm{sf}})(1+\cos^2\theta) \times$$
$$\left\{\frac{3\Gamma_{ee}\Gamma_{\mu\mu}}{\Gamma M}\mathrm{Im}\mathcal{F} - \frac{2\alpha\sqrt{\Gamma_{ee}\Gamma_{\mu\mu}}}{M}\mathrm{Re}\frac{\mathcal{F}}{1-\Pi_0}\right\}, \qquad (7)$$

where a correction δ_{sf} follows from the structure function approach of [9]:

$$\delta_{\mathrm{sf}} = \frac{3}{4}\beta + \frac{\alpha}{\pi}\left(\frac{\pi^2}{3}-\frac{1}{2}\right) + \beta^2\left(\frac{37}{96}-\frac{\pi^2}{12}-\frac{1}{36}\ln\frac{W}{m_e}\right) \qquad (8)$$

and

$$\mathcal{F} = \frac{\pi\beta}{\sin\pi\beta}\left(\frac{M/2}{-W+M-i\Gamma/2}\right)^{1-\beta} \qquad (9)$$

with

$$\beta = \frac{4\alpha}{\pi}\left(\ln\frac{W}{m_e}-\frac{1}{2}\right). \qquad (10)$$

The terms proportional to $\mathrm{Im}\mathcal{F}$ and $\mathrm{Re}\mathcal{F}$ describe the contribution of the resonance and the interference effect, respectively.

Originally in Ref. [10] the electron loops only were taken into account in Π_0 while the terms $\lesssim \beta^2$ were omitted including the $\pi\beta/\sin\pi\beta$ factor [11] in (9).

For the e^+e^- final state one has

$$\left(\frac{d\sigma}{d\Omega}\right)^{ee\to ee} \approx \left(\frac{d\sigma}{d\Omega}\right)_{\mathrm{QED}}^{ee\to ee} +$$
$$\frac{1}{M^2}\left\{\frac{9}{4}\frac{\Gamma_{ee}^2}{\Gamma M}(1+\cos^2\theta)(1+\delta_{\mathrm{sf}})\mathrm{Im}\mathcal{F} - \frac{3\alpha}{2}\frac{\Gamma_{ee}}{M}\left[(1+\cos^2\theta)-\frac{(1+\cos\theta)^2}{(1-\cos\theta)}\right]\mathrm{Re}\mathcal{F}\right\}, \qquad (11)$$

where the relative accuracy of the interference term is about β (7.6% for J/ψ). That is sufficient for the analysis reported.

For the nonresonant contribution σ_{QED} the calculations of [12, 13] can be used implemented in the event generators BHWIDE [14] and MCGPJ [15].

In order to compare the theoretical cross sections (7) and (11) with experimental data, it is necessary to perform their convolution with a distribution of the total collision energy which is assumed to be Gaussian with an energy spread σ_W:

$$\rho(W) = \frac{1}{\sqrt{2\pi}\,\sigma_W}\exp\left(-\frac{(W-W_0)^2}{2\sigma_W^2}\right),$$

---

*We are grateful to V. S. Fadin for clarification of this issue.

where W_0 is an average c.m. collision energy.

3 VEPP-4M collider and KEDR detector

The VEPP-4M collider [16] can operate in the wide range of beam energy from 1 to 6 GeV. The peak luminosity in the J/ψ energy region is about $2 \times 10^{30}\,\mathrm{cm}^{-2}\mathrm{s}^{-1}$.
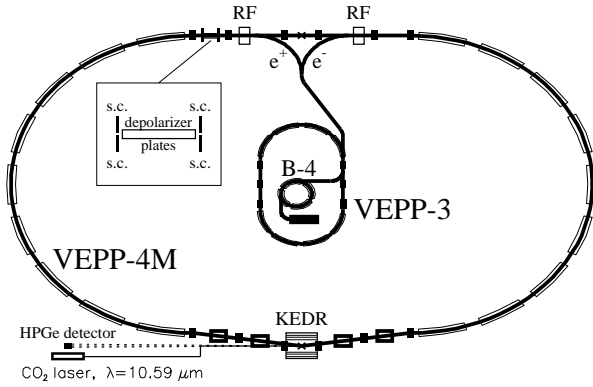

Fig. 1. VEPP-4M/KEDR complex with the resonant depolarization and the infrared light Compton backscattering facilities.

One of the main features of the VEPP-4M is a possibility of precise energy determination. The resonant depolarization method [17, 18] was implemented at VEPP-4 from the beginning of experiments in early eighties for the measurements of the J/ψ and $\psi(2S)$ mass with the OLYA [19] detector and Υ family mass with the MD-1 [19] detector.

At VEPP-4M the accuracy of the energy calibration with the resonant depolarization is improved to about 10^{-6}. The interpolation of energy between calibrations [20] in the J/ψ region has the accuracy of $6 \cdot 10^{-6}$ ($\simeq 10$ keV).

In 2005 a new technique developed at the BESSY-I and BESSY-II synchrotron radiation sources [21, 22] was adopted for VEPP-4M. It employs the infrared light Compton backscattering and has a worse precision ($50 \div 70$ keV in the J/ψ region) but, unlike the resonant depolarization, can be used during data taking.

The KEDR detector [23] includes the vertex detector, the drift chamber, the scintillation time-of-flight counters, the aerogel Cherenkov counters, the barrel liquid krypton calorimeter, the endcap CsI calorimeter, and the muon system built in the yoke of a superconducting coil generating a field of 0.65 T. The detector also includes the scattered electron tagging system for studying of the two-photon pro-

cesses. The on-line luminosity is measured by two independent single bremsstrahlung monitors.

4 Experiment description

In April 2005, the 11-point scan of the J/ψ has been performed with the integral luminosity of 230 nb^{-1}. This corresponds approximately to 15000 $J/\psi \to e^+ e^-$ decays. During this time, 26 calibrations of the beam energy were done using the resonance-depolarization method.

Single bremsstrahlung and Bhabha scattering to the endcap calorimeter were used in the relative measurement of luminosity. The absolute calibration of the luminosity was performed using the large angle Bhabha scattering in the $\Gamma_{ee} \times \Gamma_{ee}/\Gamma$ analysis.
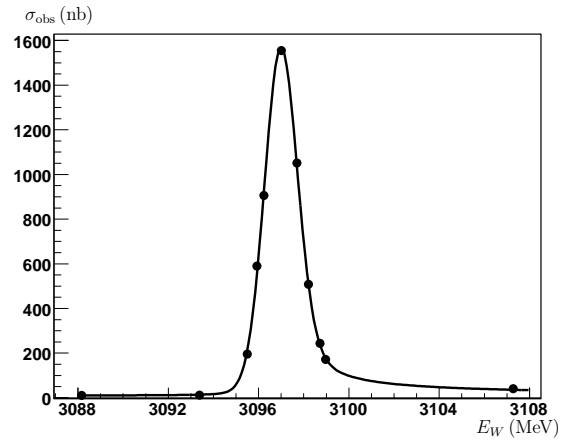

Fig. 2. Observed $e^+ e^- \to$ hadrons cross section according to the results of the J/ψ scan.

Figure 2 shows the observed $e^+ e^- \to$ hadrons cross section at the J/ψ energy region. These data were used to fix the resonance peak position and to determine the beam energy spread. The value of the J/ψ mass agrees with the earlier VEPP-4M/KEDR experiments [20].

5 Data analysis

In our analysis we employed the simplest selection criteria that ensured a sufficient suppression of multi-hadron events and the cosmic-ray background, please see Ref. [24] for details.

In order to measure the resonance parameters in the $e^+ e^-$ channel, the set of events was divided into ten equal angular intervals from 40° to 140°. At the i-th point in energy E_i and the j-th angular interval θ_j, the expected number of events was parameterized

as

$$N_{\exp}(E_i,\theta_j) = \mathcal{R}_{\mathcal{L}} \times \mathcal{L}(E_i) \times$$
$$\Big(\sigma_{\text{res}}^{\text{theor}}(E_i,\theta_j) \cdot \varepsilon_{\text{res}}^{\text{sim}}(E_i,\theta_j) +$$
$$\sigma_{\text{inter}}^{\text{theor}}(E_i,\theta_j) \cdot \varepsilon_{\text{inter}}^{\text{sim}}(E_i,\theta_j) + \qquad (12)$$
$$\sigma_{\text{Bhabha}}^{\text{sim}}(E_i,\theta_j) \cdot \varepsilon_{\text{Bhabha}}^{\text{sim}}(E_i,\theta_j) \Big).$$

where $\mathcal{L}(E_i)$ is the integrated luminosity measured by luminosity monitor at the i-th point; $\sigma_{\text{res}}^{\text{theor}}$, $\sigma_{\text{inter}}^{\text{theor}}$ and $\sigma_{\text{Bhabha}}^{\text{theor}}$ are the theoretical cross sections respectively for resonance, interference and Bhabha contributions; $\varepsilon_{\text{res}}^{\text{sim}}$, $\varepsilon_{\text{inter}}^{\text{sim}}$ and $\varepsilon_{\text{Bhabha}}^{\text{sim}}$ are detector efficiencies obtained from simulated data.

In this formula the following free parameters were used:

1. the product $\Gamma_{ee} \times \Gamma_{ee}/\Gamma$, which determines the magnitude of the resonance signal;

2. the electron width Γ_{ee}, which specifies the amplitude of the interference wave;

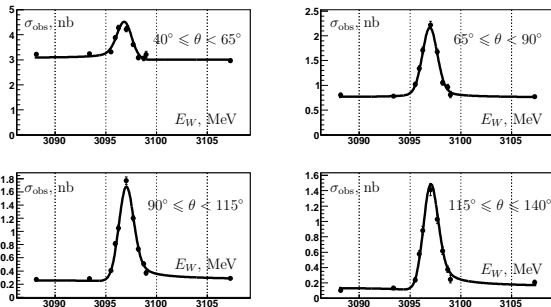3. the coefficient $\mathcal{R}_{\mathcal{L}}$, which provides the absolute calibration of the luminosity monitor.

Fig. 3.   Fits to experimental data for $e^+e^- \to e^+e^-$ process at J/ψ energy region for four angular ranges.

We note that the coefficient $\mathcal{R}_{\mathcal{L}}$ partially accounts the possible difference between the actual detection efficiency and simulation in the case where these difference do not depend on the scattering angle or the beam energy (or the data taking time) thus the substantial cancellation of errors occurs.

Figure 3 shows our fit to the data for four angular intervals. The joined fit in ten equal intervals from $40°$ to $140°$ produce the following basic result:

$$\Gamma_{ee} \times \Gamma_{ee}/\Gamma = 0.3323 \pm 0.0064\,(\text{stat.})\,\text{keV},$$
$$\mathcal{R}_{\mathcal{L}} = 93.4 \pm 0.7\,(\text{stat.})\,\%,$$
$$\Gamma_{ee} = 5.7 \pm 0.6\,(\text{stat.})\,\text{keV}. \qquad (13)$$

Due to different angular distributions for Bhabha scattering and resonance events, subdivision of the

data into several angular bins decreases a statistical error for $\Gamma_{ee} \times \Gamma_{ee}/\Gamma$ by $40 \div 50\%$. The electron width obtained by the fit has a statistical error of about 10% and agrees with the world-average value.
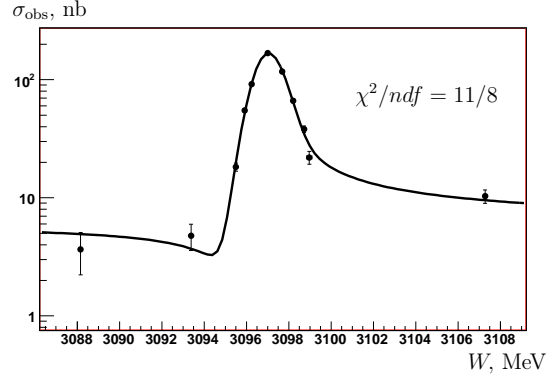
Fig. 4.   Fit to experimental data for $e^+e^- \to \mu^+\mu^-$ process at J/ψ energy region.

Similarly to (12), the expected number of $e^+e^- \to \mu^+\mu^-$ events was parameterized in the form:

$$N_{\exp}(E_i) = \mathcal{R}_{\mathcal{L}} \times \mathcal{L}(E_i) \times$$
$$\Big(\sigma_{\text{res}}^{\text{theor}}(E_i) \cdot \varepsilon_{\text{res}}^{\text{sim}}(E_i) +$$
$$\sigma_{\text{inter}}^{\text{theor}}(E_i) \cdot \varepsilon_{\text{inter}}^{\text{sim}}(E_i) + \qquad (14)$$
$$\sigma_{\text{bg}}^{\text{theor}}(E_i) \cdot \varepsilon_{\text{bg}}^{\text{sim}}(E_i) \Big) + F_{\text{cosmic}} \times T_i,$$

with the same meaning of $\mathcal{R}_{\mathcal{L}}$ and $\mathcal{L}(E_i)$ as in (12). $\mathcal{L}(E_i)$ is multiplied by the sum of the products of theoretical cross sections for resonance, interference and QED background and detection efficiencies as obtained from simulated data. $\mathcal{R}_{\mathcal{L}}$ was fixed by result (13). T_i is the live data taking time. Unlike (12) there is only one angular interval from $40°$ to $140°$.

The following free parameters were used:

1. the product $\Gamma_{ee} \times \Gamma_{\mu\mu}/\Gamma$, which determines the magnitude of the resonance signal;

2. the square root of electron and muon widths $\sqrt{\Gamma_{ee}\Gamma_{\mu\mu}}$, which specifies the amplitude of the interference wave;

3. the cosmic events rate F_{cosmic} passed the selection criteria for the $e^+e^- \to \mu^+\mu^-$ events.

Due to variations of luminosity during the experiment it is possible to separate cosmic events contribution ($F_{\text{cosmic}} \cdot T_i$) from nonresonant background contribution ($\sigma_{\text{bg}}^{\text{theor}}(E_i) \cdot \varepsilon_{\text{bg}}^{\text{sim}}(E_i) \cdot L_i$).

Figure 4 shows our fit to the $e^+e^- \to \mu^+\mu^-$ data. It yields the following result:

$$\Gamma_{ee} \times \Gamma_{\mu\mu}/\Gamma = 0.3318 \pm 0.0052\,(\text{stat.})\,\text{keV},$$
$$\sqrt{\Gamma_{ee} \times \Gamma_{\mu\mu}} = 5.6 \pm 0.7\,(\text{stat.})\,\text{keV}. \qquad (15)$$

As can be seen from (15) the statistical error of $\Gamma_{ee} \times \Gamma_{\mu\mu}/\Gamma$ is about 1.6%.

6 Discussion of systematic uncertainty

The most significant systematic uncertainties in the $\Gamma_{ee} \times \Gamma_{ee}/\Gamma$ and $\Gamma_{ee} \times \Gamma_{\mu\mu}/\Gamma$ measurements are listed in Tables 1 and 2, respectively.

Table 1.   Systematic uncertainties in $\Gamma_{ee} \times \Gamma_{ee}/\Gamma$.

Systematic uncertainty source	Error %
Luminosity monitor instability	0.8
Offline event selection	0.7
Trigger efficiency	0.5
Energy spread accuracy	0.2
Beam energy measurement (10–30 keV)	0.3
Fiducial volume cut	0.2
Calculation of radiative correction	0.2
Cross section for Bhabha (MC generators)	0.4
Uncertainty in the final state radiation (PHOTOS)	0.4
Background from J/ψ decays	0.2
Fitting procedure	0.2
Quadratic sum	*1.4*

Table 2.   Systematic uncertainties in $\Gamma_{ee} \times \Gamma_{\mu\mu}/\Gamma$.

Systematic uncertainty source	Error %
Luminosity monitor instability	0.8
Absolute luminosity calibration by e^+e^- data	1.2
Trigger efficiency	0.5
Energy spread accuracy	0.4
Beam energy measurement (10–30 keV)	0.5
Fiducial volume cut	0.2
Calculation of radiative correction	0.1
Uncertainty in the final state radiation (PHOTOS)	0.5
Nonresonant background	0.1
Background from J/ψ decays	0.6
Quadratic sum	*1.8*

A rather large uncertainty of 0.8% common for the electron and muon channels is due to the luminosity monitor instability. It was estimated from comparing the results obtained using the on-line luminosity of the single bremsstrahlung monitor and the off-line luminosity measured by the e^+e^- scattering in the endcap calorimeter.

The essential source of uncertainty is an imperfection of the detector response simulation resulting in the errors in the trigger and offline event selection efficiencies. It was studied using collected data and the correction of $0.75 \pm 0.7\%$ was applied.

The dominant uncertainty of the $\Gamma_{ee} \times \Gamma_{\mu\mu}/\Gamma$ result is associated with the absolute luminosity calibration done in e^+e^--channel. It includes the accuracy of the Bhabha event generators, the statistic error of $\mathcal{R}_{\mathcal{L}}$ parameter (13) and the residual (after correction using simulated data) efficiency difference for e^+e^- and $\mu^+\mu^-$ events. The additional correction applied to this difference is $-0.5 \pm 0.9\%$.

The other sources of uncertainty are discussed in Ref. [24].

7 Results and Conclusion

The new measurement of the $\Gamma_{ee} \times \Gamma_{ee}/\Gamma$ and $\Gamma_{ee} \times \Gamma_{\mu\mu}/\Gamma$ has been performed at the VEPP-4M collider using the KEDR detector. The following results have been obtained (in keV):

$$\Gamma_{ee} \times \Gamma_{ee}/\Gamma = 0.3323 \pm 0.0064\,(\text{stat.}) \pm 0.0048\,(\text{syst.})$$
$$\Gamma_{ee} \times \Gamma_{\mu\mu}/\Gamma = 0.3318 \pm 0.0052\,(\text{stat.}) \pm 0.0063\,(\text{syst.})$$
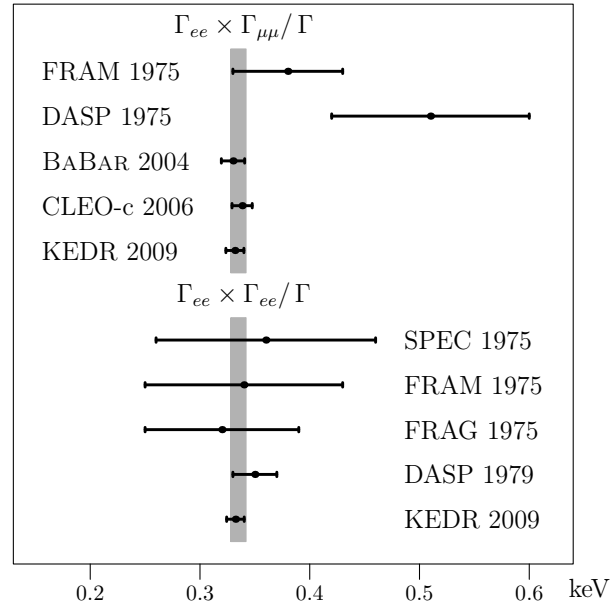

Fig. 5.   Comparison of $\Gamma_{ee} \times \Gamma_{ee}/\Gamma$ and $\Gamma_{ee} \times \Gamma_{\mu\mu}/\Gamma$ measured at different experiments mentioned in [25] with KEDR 2009 results. The vertical strip is for the world average $\Gamma_{ee} \times \Gamma_{\mu\mu}/\Gamma$ value.

Figure 5 shows the comparison of our results with those of the previous experiments. The grey line shows PDG average and the error for the $\Gamma_{ee} \times \Gamma_{\mu\mu}/\Gamma$ product measurement. The new KEDR results are the most precise. Results are in good agreement with each other and with the world average value of $\Gamma_{ee} \times \Gamma_{\mu\mu}/\Gamma$.

Accounting the correlations in the $\Gamma_{ee} \times \Gamma_{ee}/\Gamma$ and $\Gamma_{ee} \times \Gamma_{\mu\mu}/\Gamma$ errors the mean value is

$$\Gamma_{ee} \times \Gamma_{\ell\ell}/\Gamma = 0.3320 \pm 0.0041\,(\text{stat.}) \pm 0.0050\,(\text{syst.})\,\text{keV}.$$

With the assumption of lepton universality and using independent data on branching fraction $\mathcal{B}(J/\psi \to e^+e^-) = (5.94 \pm 0.06)\,\%$ [25] leptonic and full widths of J/ψ meson were determined:

$$\Gamma_{\ell\ell} = 5.59 \pm 0.12\,\text{keV}$$
$$\Gamma = 94.1 \pm 2.7\,\text{keV}$$

These results are in good agreement with the world average [25] and with the results from BaBar [5] and CLEO-c [6] experiments.

References

1 A. M. Badalian and I. V. Danilkin, Di-electron and two-photon widths in charmonium, 2008, arXiv:0801.1614.

2 O. Lakhina and E. S. Swanson, Physical Review D **74**, 014012 (2006), arXiv:hep-ph/0603164.

3 J. J. Dudek, R. G. Edwards, and D. G. Richards, Physical Review D **73**, 074507 (2006), arXiv:hep-ph/0601137.

4 N. Brambilla *et al.*, Heavy quarkonium physics, 2005, arXiv:hep-ph/0412158.

5 B. Aubert and The BABAR Collaboration, Physical Review D **69**, 011103 (2004), arXiv:hep-ex/0310027.

6 G. S. Adams and C. Collaboration, Physical Review D **73**, 051103 (2006), arXiv:hep-ex/0512046.

7 KEDR, V. V. Anashin *et al.*, Nucl. Phys. Proc. Suppl. **181-182**, 353 (2008).

8 Y.-S. Tsai, Presented at Asia Pacific Physics Conf., Singapore, Jun 12- 18, 1983.

9 E. A. Kuraev and V. S. Fadin, Sov. J. Nucl. Phys. **41**, 466 (1985).

10 Y. I. Asimov *et al.*, Pisma Zh. Eksp. Teor. Fiz. **21**, 378 (1975), [Ya. I. Asimov et al., JETP Lett. **21**, 172 (1975)].

11 K. Y. Todyshev, (2009), arXiv:0902.4100.

12 W. Beenakker, F. A. Berends, and S. C. van der Marck, Nucl. Phys. **B349**, 323 (1991).

13 A. B. Arbuzov *et al.*, JHEP **9710**, 001 (1997).

14 S. Jadach, W. Płaczek, and B. F. L. Ward, Phys. Lett. B **390**, 298 (1997), UTHEP-95-1001.

15 A. B. Arbuzov, G. V. Fedotovich, F. V. Ignatov, E. A. Kuraev, and A. L. Sibidanov, Eur. Phys. J. **C46**, 689 (2006), arXiv:hep-ph/0504233.

16 V. Anashin *et al.*, Stockholm 1998, EPAC 98* , 400 (1998), Prepared for 6th European Particle Accelerator Conference (EPAC 98), Stockholm, Sweden, 22-26 Jun 1998.

17 A. D. Bukin *et al.*, IYF-75-64.

18 A. N. Skrinsky and Y. M. Shatunov, Sov. Phys. Usp. **32**, 548 (1989).

19 OLYA, A. S. Artamonov *et al.*, Phys. Lett. B **474**, 427 (2000), arXiv:hep-ex/0001040.

20 KEDR, V. M. Aulchenko *et al.*, Phys. Lett. B **573**, 63 (2003), arXiv:hep-ex/0306050.

21 R. Klein, R. Thornagel, G. Ulm, T. Mayer, and P. Kuske, Nucl. Instrum. Meth. **A384**, 293 (1997).

22 R. Klein *et al.*, Nucl. Instrum. Meth. **A486**, 545 (2002).

23 V. V. Anashin *et al.*, Nucl. Instrum. Meth. **A478**, 420 (2002).

24 KEDR, V. V. Anashin *et al.*, (to be published in Phys. Lett. B), arXiv:0912.1082.

25 Particle Data Group, C. Amsler *et al.*, Phys. Lett. **B667**, 1 (2008).